



Self-assembling peptide nanofiber scaffolds for controlled release governed by gelator design and guest size

Ying Zhao ^{a,b}, Masayoshi Tanaka ^a, Takatoshi Kinoshita ^{a,*}, Masahiro Higuchi ^a, Tianwei Tan ^{b,*}

^a Department of Materials Science and Engineering, Graduate School of Engineering, Nagoya Institute of Technology, Gokiso-cho, Showa-ku, Nagoya 466-8555, Japan

^b College of Life Science and Technology, Beijing University of Chemical Technology, 15 Beisanhuan East Road, Chaoyang District, Beijing 100029, China

ARTICLE INFO

Article history:

Received 8 June 2010

Accepted 6 August 2010

Available online 13 August 2010

Keywords:

Drug release

Nanostructure

Peptide

Scaffold

Self-assembly

ABSTRACT

The aim of this study was to develop controlled drug delivery by network scaffolds based on self-assembling peptide RADAII and RADAII. These two peptides self-assembled into interconnected nanofibrillar network structures with distinct physical morphologies. The hydrogels were also utilized for entrapment and release of some model guests, promising their future application as a drug delivery vehicle. Fickian diffusion controlled the release kinetics. Furthermore, the obtained release function was dependent on both rational design of the peptides used for hydrogel formation and choice of the entrapped molecules. On the basis of the striking different releases of these two peptide scaffolds, we suggested that guest size and lipophilicity influenced the release competitively. The release of RADAII system was dominated by guest size, and the guest lipophilicity controlled the release behavior in RADAII system. In a word, this work would potentially provide a spatially and temporally controlled delivery system for some functional drugs in the future.

© 2010 Elsevier B.V. All rights reserved.

1. Introduction

Hydrogels are usually based on physical or chemical crosslinks of hydrophilic gelators to form a three-dimensional network [1,2]. It is able to immobilize and entrap large amounts of water resulting in tissue-mimicking environment [3–5]. Compared to hydrogels prepared using polymers, research related to fibrous network structures prepared from peptides through self-assembly has been rapidly expanding in recent years [6–10]. Intriguingly, some excellent properties of peptide-based hydrogels represent considerable potential in various biomedical applications [6,7,11–14]. Especially, such hydrogels can be formed *in situ*, and they have also the ability to bind and store biomolecules and release them, which make the hydrogels particularly suitable as drug delivery systems [15–17]. Here, it should be pointed out that an extraordinary benefit of using self-assembling hydrogels is realized during the formulation of drug-loaded material. In principle, compared with methods where a drug is diffused into a preformed gel, precise concentrations of therapeutics can be encapsulated directly within the scaffold during the self-assembly process, which can enable prolonged activity if the release rate of the drug can be controlled [11,18].

To the best of our knowledge, one of the significant advantages of supramolecular materials is that appropriate design of small building molecules allows efficient control over the assembled structure and

its function [19]. Our research efforts were directed to search for the oligopeptide that can form hydrogel phase materials by their self-assembly [20–23]. In the course of our continuing investigation, it is recently demonstrated that hydrogels can be prepared in the presence of guest molecules using two L-peptides, RADAII ($[CH_3CONH]-RADARADFRADARADA-[CONH_2]$) and RADAII ($[CH_3CONH]-RADFRADARADA-[CONH_2]$). We are interested in making a variant of RADAII by changing the position of phenylalanine residue and addressing the question of whether this molecule can self-assemble into an ordered manner to form a hydrogel. Our main intention of this alteration is to change $\pi-\pi$ stacking morphology in self-assembly. It has been found that these two nanofiber hydrogels showed distinct nanostructures and macroscopical properties [20], and they had great potential for chiral separation [21].

As controlled drug release enters into more and more applications in medicine, there is a growing interest in developing a system that is amenable to molecular design and can be tailor made for the specific drugs. As far as we are concerned, it has been reported that the guest size plays an important role in determining the biological response of the tissue to foreign biomaterials [24,25]. In addition, the different releases of guests with various sizes from the hydrogel scaffolds displaying different nanostructures have not been reported in the literature yet. Therefore, in the present study, we expand on the previous work by focusing on understanding whether conjugation of guests with various molecular sizes to RADAII and RADAII hydrogels would influence the physical properties of materials. To explore the effects of phenylalanine residue positioning on the entrapment and release, phenylalanine (Phe), tryptophan (Trp), and phenol red (PR) were used as model guest molecules. To investigate this topic is

* Corresponding authors. Kinoshita is to be contacted at Tel./fax: +81 52 735 5267. Tan, Tel./fax: +86 10 6441 6691.

E-mail addresses: kinoshita.takatoshi@nitech.ac.jp (T. Kinoshita), twtan@mail.buct.edu.cn (T. Tan).

therefore not only interesting for the potential use of such systems as drug delivery vehicles, but potentially also for understanding the self-assembling mechanisms of such peptide scaffolds better.

2. Materials and methods

2.1. Materials

The amphiphilic peptides, RADAII and RADAII, were synthesized by a standard solid-phase peptide synthetic strategy following a standard Fmoc-protection protocol, using 433 Peptide Synthesizer (Applied Biosystems Inc., CA, USA), and was confirmed by using matrix-assisted laser desorption ionization time-of-flight mass spectrometry (MALDI-TOF MS) [20]. For applications, the N- and C-terminals were both derivatized. Phe, Trp, and PR were purchased from Nacalai Tesque, Inc. (Tokyo, Japan) and dissolved in Milli-Q water to prepare solutions at a concentration of 1 mM. The other reagents were obtained commercially and used without further purification.

2.2. Preparation of peptide scaffolds

Phe (MW: 165.19), Trp (MW: 204.23), and PR (MW: 354.38) were used as model guest molecules (supporting data, Table S1). Peptide and guest were mixed in Milli-Q water and Tris-HCl buffer (pH 7.4), and the final concentrations of peptides and guests in the mixture were 0.5 (w/v)% (5 mg/mL; 2.8 mM) and 1 mM, respectively. The peptides self-assembled in the aqueous solution containing guests into higher-order nanofiber hydrogels with extremely high water content. Self-supporting hydrogels were defined as those that remain attached to the bottom of the vial for at least 30 s with little or no observable viscous flow, when inverting the container [26,27].

2.3. CD measurement

Circular dichroism (CD) spectra were obtained using a JASCO J-820K spectropolarimeter which was flushed with nitrogen during operation. Wavelength scans were recorded at 0.1 nm intervals from 260 to 190 nm, using a 0.1 mm path length quartz cuvette. The spectra obtained were averaged from 16 consecutive scans and subtracted from the background. Ellipticity measurement was shown to mean residue ellipticity ($[\theta]$, in deg cm² dmol⁻¹).

2.4. Rheological characterization

Viscoelastic property was determined by using a rheometer (AR1000, TA Instruments), and a 40-mm-diameter stainless-steel parallel plate was used. Viscoelastic properties of samples were conducted by loading 310 μ L of the freshly prepared samples on the sample platform of the instrument, followed immediately by a series of rheometrical tests at 25 °C. For the determination of viscoelastic properties and to avoid the influence of mixing and breakdown during loading for samples, they were immediately subjected to a 3 h time sweep test. After the data reached a well-defined equilibrium, a series of frequency sweep tests and strain amplitude sweep tests were sequentially carried out. Dynamic time sweep experiments were performed with a frequency and strain amplitude of 6 rad/s and 0.1, respectively. The oscillatory frequency sweep tests (frequency $\omega=0.1\text{--}100$ rad/s) were studied to measure G' and G'' , the linear viscoelastic storage and loss modulus, respectively. The oscillatory strain amplitude sweep tests (strain amplitude $\gamma_0=0.001\text{--}10$) at a fixed frequency (6 rad/s) were investigated.

2.5. AFM observation

Mica, having a freshly cleaved surface, was inserted into hydrogel. After about 15 s, the hydrogel on the mica was washed by Milli-Q water (50 μ L), and then the mica was air-dried for 24 h. The images were obtained by scanning the mica surface in air by AFM (Nanoscope IIIa, Digital Instruments, Santa Barbara, CA) using a silicon cantilever (NCHV-10 V, Veeco Instruments) operated in tapping mode. This tip (ADV: 42 N/m, 320 kHz, no coating) is one of the most highly used probes for tapping mode in air.

2.6. Release study

Peptides RADAII and RADAII self-assembled into hydrogels in the aqueous solutions including model guests. 500 μ L of the hydrogel was placed at the bottom of quartz cell (12.5 mm × 12.5 mm × 45 mm) and the hydrogel formed overnight at room temperature. Then, 2.5 μ L of Tris-HCl buffer (pH 7.4) was slowly added to each cell so as to not disrupt the hydrogel structure. The *in vitro* release studies were performed at 25 °C, where the supernatant guest concentration was measured every about 30 min.

The concentration of the guest molecules in the supernatant was quantitatively determined by a UV-visible spectrophotometer (JASCO V-550). The amount of the guest released from the hydrogel was measured using a calibration curve of the pure guest in Tris-HCl buffer (pH 7.4) at the wavelength where they showed their maximum absorbance (Phe: 257.5 nm, Trp: 279.5 nm, and PR: 429 nm). The averages from five independent determinations were plotted.

In addition, over the time course of the experiment, this gel/solution two-phase system was still stable, and no obvious volume change occurred. And it is noticeable that the release data obtained in our experiments had already removed the interference coming from the change. Here, the release ratio were calculated by

$$\text{Release ratio} = \frac{M_t}{M_\infty} \quad (1)$$

where M_∞ and M_t represent the initial amount of guest loaded and the cumulative amount of guest released at time t [28].

3. Results and discussion

Here, guest size and nanofiber structures of hydrogels were varied to establish the potential use of these materials as drug delivery matrices. To achieve this application, it is essential to investigate basic physical-chemical properties of the hydrogels. With the ultimate aim to select optimal design for special encapsulation/release applications, in this manuscript, we first physically and chemically characterized the hydrogels. Next, we stated the different release behaviors of the guests with various sizes.

3.1. Secondary structure in peptide systems

CD spectroscopy was used to monitor the extent of β -sheet secondary structure for RADAII and RADAII in various solvent systems. For both peptides, a clear minimum at 216 nm was observed along with a maximum near 195 nm (Fig. 1). In all cases, the CD spectra had been accepted as being consistent with β -sheet rich structures. Also, adding guests did not immediately change the β -sheets, which also supported the importance of the internal order in the nanofibers [29].

It was interesting to find that with guest size, as a consequence of RADAII self-assembly, a progressive structural evolution to an obvious β -sheet conformation was observed in the solution of PR (Fig. 1a). RADAII also adopted strong β -sheet spectroscopic signatures in each of the solvent systems (Fig. 1b). After adding guests, the

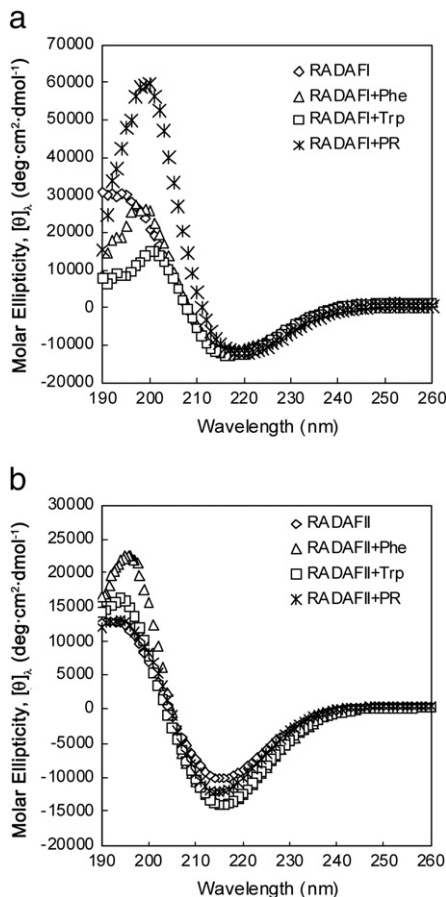


Fig. 1. CD spectra for the secondary structure of peptide (a) RADAII and (b) RADAII with various guests: (◊) no guest; (△) Phe; (□) Trp; (*) PR.

β -sheet content of RADAII systems enhanced. This finding suggested an increase in aggregate content and/or a larger order of the existing β -sheet aggregates resulting in a higher dichroic activity. To the best of our knowledge, hydrophobic side chains contributed significantly to the stability of β -sheet structures [30]. Consistent with this model, we suggested that guest had an important role in RADAII self-assembly due to its location in the hydrophobic area of peptide nanofiber, so that the peptide could easily assemble. However, the guest sensitivity of the secondary structure in RADAII systems was significantly reduced and the β -sheets were stabilized (Fig. 1a). No increase in the intensity of the minimum at 216 nm was found after adding guest. When explaining the insensitivity of peptide RADAII to guest changes, the steric hindrance effect should also be considered.

3.2. Nanostructures of peptide nanofiber scaffolds

To visualize the morphological features of the self-assembling nanostructures of each peptide after adding guests, we used AFM analysis which enables *in situ* imaging of the hydrogel matrix. All peptides that formed hydrogels were arranged as consistent nanofibrous network structures (Fig. 2). Moreover, the physical crosslinks was pronounced in the peptide hydrogels, and these structures coincided with the mechanism of network formation. Fibril formation occurred when the hydrophobic residues of neighboring peptides collapsed together to exclude water and subsequently underwent further assembly into fibrils through hydrogen-bond [31]. Each long fiber might be connected from the short fibrillar fragments which arose from smaller assemblies such as peptide stacks [32].

The morphology was strongly dependent on the composition of the hydrogels. Although both formed fibers, the two formulations

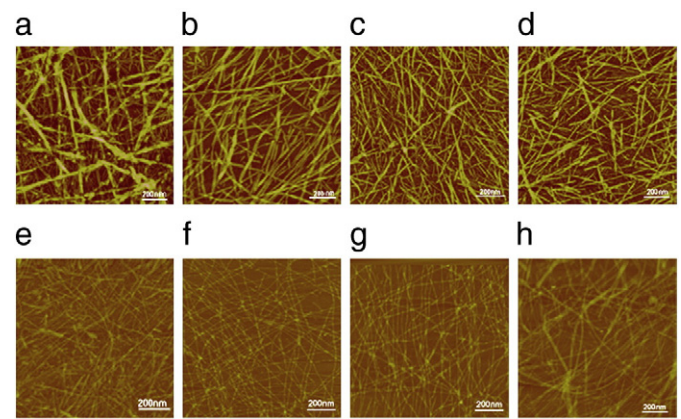


Fig. 2. Tapping-mode AFM images (scale: 200 nm; image size: 1 $\mu\text{m} \times 1 \mu\text{m}$; Z scale: 20 nm) obtained from (a) RADAII scaffold, (b) RADAII scaffold loading Phe, (c) RADAII scaffold loading Trp, (d) RADAII scaffold loading PR, (e) RADAII scaffold, (f) RADAII scaffold loading Phe, (g) RADAII scaffold loading Trp, and (h) RADAII scaffold loading PR.

showed the striking discrepancy of nanofiber morphology in scaffolds. As discussed previously [20], the RADAII networks were clearly composed of close-packed and twisted fibers which were bundled up to give an average diameter ranging from 10 to 40 nm and extended lengths approaching many micrometers (Fig. 2a). Noteworthy, shorter and thinner fibers were obtained in RADAII networks by addition of guests (Fig. 2b-d), typically observed as several hundred nanometers or less in length and 8–15 nm in diameter. On the other hand, RADAII showed the presence of an organized network of a population of singular and untwisted fibrils with a well-defined and highly uniform width. Compared with the coexistence of short and long fibrils in individual RADAII network (Fig. 2e), the fibrils appeared to have a homogeneous persistence length after adding guests into RADAII scaffolds (Fig. 2f-h). And despite the increase in length, the fibrillar diameter was not observed to significantly change. Our observations demonstrated that we could control fiber dimension and aggregation by addition of guests.

Probably the morphology was assisted by the nature of self-assembling structure [33]. These observations supported the notion that there might be interesting structural effects depending on aromatic interactions in the self-assembly process of the peptides [34], which was supported by previous studies [20]. Thus, we speculated on that the location of the aromatic groups in the peptide chain had a direct influence on the structure of the self-assembled product [20].

3.3. Mechanical properties of peptide nanofiber scaffolds

The mechanical properties of the peptide hydrogels are important for determining their suitability in various applications [35]. Hence, the gelation behavior of the peptides was investigated rheologically in order to determine the nature of the hydrogel networks being formed [6]. The rheological analysis showed how the location of aromatic groups on the peptide backbone and the addition of model guest affected the mechanical properties of the respective hydrogel.

RADAII and RADAII gelation behavior and their mechanical properties differed in a number of significant respects. The storage modulus (G') is an indicator of elastic behavior and measures the ability to store deformation energy that can be recovered after removing the load cycle [36]. The RADAII systems with guest exhibited greater values of G' than that of the hydrogel without guest (Fig. 3b), indicating that more stable hydrogels were formed. While aromatic interactions were clearly not necessary for self-assembly, these observations implied that there might be interesting structural effects based on aromatic interactions. Greater G' also suggested strong $\pi-\pi$ interactions between guest and phenyl groups

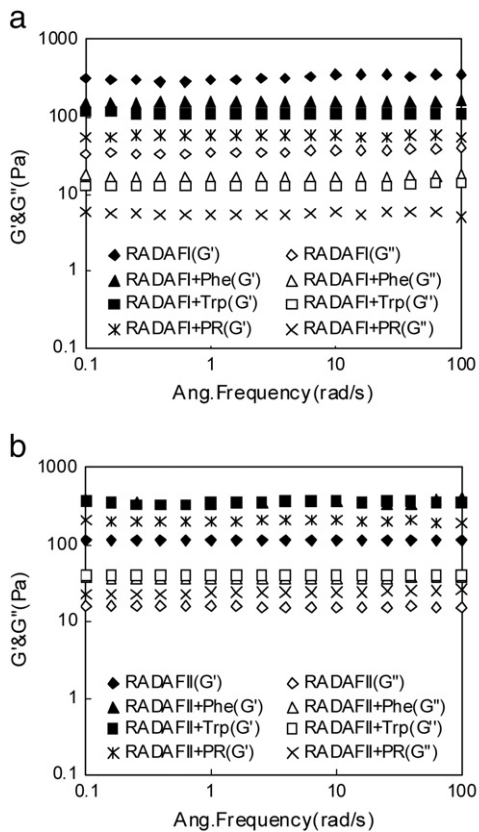


Fig. 3. Storage modulus (G') and loss modulus (G'') as frequency sweeps for (a) RADAFI and (b) RADAFII hydrogels loading various guests. The concentrations of peptide and guest were 0.5 (w/v)% and 1 mM, respectively.

of RADAFII favorable for the reinforcement of nanofiber networks [26]. These changes in the mechanical properties were also manifested through their clear differences in nanofiber length observed in networks, which, in turn, affected the corresponding network structure. Hence, the higher modulus of RADAFII scaffolds having guest could be attributed to their longer nanofibers indicated in the AFM images (Fig. 2e–h).

RADAFI hydrogel without guest showed a stronger gelation property than the other scaffolds including guest (Fig. 3a). And as guest size increased, the storage modulus of RADAFI scaffolds decreased. The different results from these two systems were consistent with the aromatic nature of the peptides. Peptide RADAFI just had one line of aromatic moieties on one backbone [20]; hence, this was possibly owing to steric hindrances caused during the self-assembly of π - π stacking by adding the bulky guest. However, peptide RADAFII contained two distinct lists of π - π stacking and more easily accepted large guest. In order to understand how guests interacted with peptide nanofibers in these two peptide systems, and how the resulting π - π stacking units further self-assembled into nanofibers and networks, Fig. 4 was used as structural models to illustrate the differences in their hierarchical self-assembling behaviors after adding guests. Above phenomena were believed to occur because the guests closest to the hydrophobic nanofiber core had been shown as the most critical for forming higher-order peptide assemblies [37,38]. Anyway, the resulting effect of controlling the mechanical modulation of the peptide-based hydrogels has many potential benefits for biomedical application [37].

Also, as seen in Fig. 3, no crossover could be detected within the 0.1–100 rad/s frequency range, and the elastic moduli were essentially frequency independent. Such rheological behavior suggested the presence of permanent junction points as opposed to transient entanglements leading to a viscoelastic plateau modulus [39]. Both

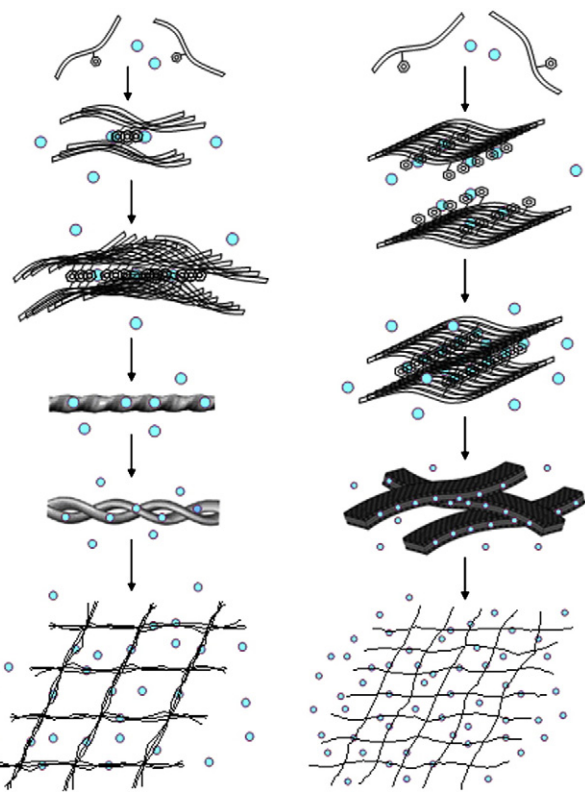
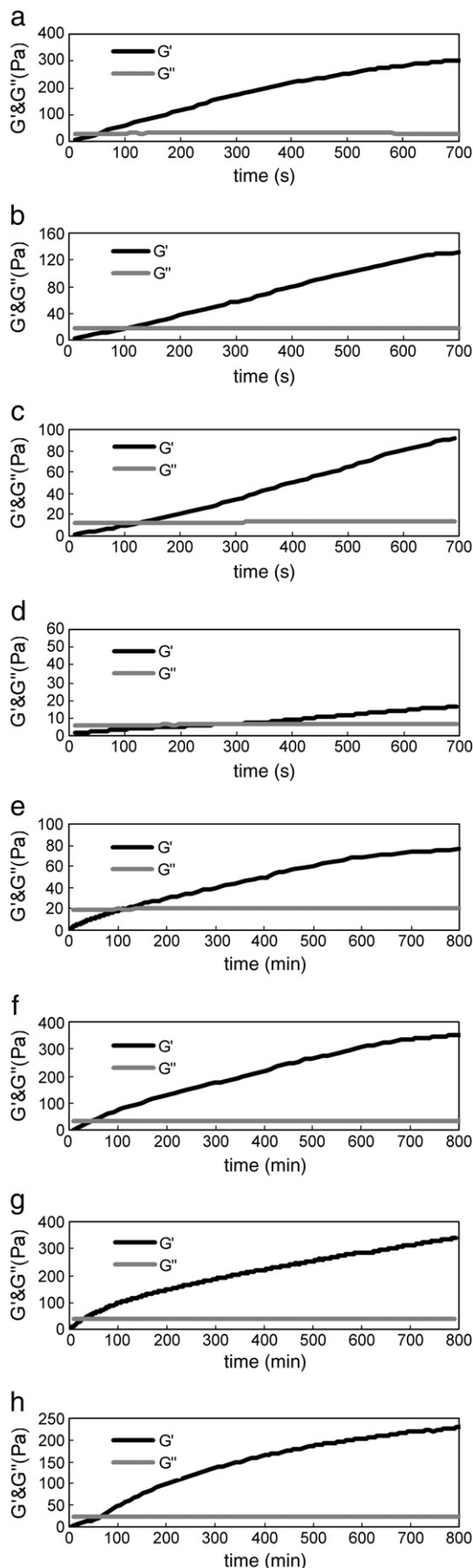


Fig. 4. Schematic illustration summarizing the nanofabrication of three-dimensional architectures by the self-assembly of peptides (left) RADAFI and (right) RADAFII after adding guests. Through controlling the functional phenyl position, a wide variety of nanostructures could be spontaneously constructed in these molecular systems.

peptide systems showed the classic response of a strong network, with a storage modulus which was nearly independent of frequency and almost an order of magnitude greater than the loss modulus.

Turning to the time dependence of the moduli of the two systems, we again found striking differences. RADAFI hydrogels required a little more prolonged time for the optical gelation after addition of guest, even though an onset of gelation of the individual peptide scaffold occurred after 1 min and a final plateau modulus took more than 10 min to develop (Fig. 5a–d). The opposite behavior was observed for the RADAFII systems including guest (Fig. 5e–h), which required less than 1 h for gelation, where the individual peptide network showed an optical transition after 2 h. We hypothesized that the time required for the optical transition corresponded to the duration of the molecules initial organization from many irregular aggregates of dimension at the range of the visible wavelength, into a crystalline form, through the process of self-assembly [35]. Thus, it seems that the distinct kinetics of the two scaffold systems might be the result of the intricacies of forming more complex supramolecular structures after addition of guest.

Self-assembling hydrogels might exhibit recovery behavior after a mechanical force. Here, an application of strain force to the hydrogel could result in the disruption of some of the physical crosslinks which define the network. This converts the mechanically rigid hydrogel into a low viscosity one capable of flow. However, when the force is removed, the physical crosslinks reform, and the hydrogel recovers its mechanical properties. Strain amplitude sweeps of the scaffolds revealed that G' decreased rapidly above a critical strain amplitude (γ_{oc}), indicating a breakdown of any physical crosslinking points by the strain (Fig. 6) [22]. All of RADAFI and RADAFII hydrogels collapsed at strains of 0.2–1.0, which might imply that the peptide nanofibers themselves were very flexible and hence able to withstand large deformations.



Even more importantly for biomedical applications [37], RADAFl systems underwent strain force and, after 3 min, recovered approximately 95% of their mechanical strength. This was in contrast to RADAFII scaffolds, which recovered only about 85% of their original storage modulus (Table 1). This recovery behavior might prove beneficial in the development of injectable hydrogel materials which could be delivered with spatial resolution from a syringe [40,41]. In application of dispensing hydrogels through a narrow bore syringe, guest containing RADAFl systems were able to be more easily dispensed and quickly regain their hydrogel characteristics.

3.4. Controlled release governed by gelator design and guest size

We quantified the release of the model guests from these peptide hydrogels. Fig. 7 showed the release curve as a plot of release ratio as a function of releasing time. In RADAFl systems, the larger size of guest accelerated its release (Fig. 7a). Due to the steric hindrance effect, larger guest was hard to locate in the hydrophobic area of nanofibers, although it showed higher lipophilicity. More of larger guests had to suspend in the hydrophilic space between crosslinking points as free molecules; therefore, they were easily released from RADAFl scaffolds.

On the other hand, the cumulative releases of three drugs were markedly distinct in RADAFII systems. For Phe, Trp, and PR, the release ratios for 24 h were 0.17, 0.12, and 0.07, respectively (Fig. 7b). Small release from the hydrogels was observed, and PR was retained in scaffolds to a greater extent than other two guests, most likely because of specific interactions between guests and peptide nanofibers [6]. Compared with the release behaviors from RADAFl scaffolds, the opposite release trend for RADAFII hydrogels at the same time interval indicated that both scaffolds were susceptible to the guest size and lipophilicity. Because there were more spaces between phenyl groups of peptide backbone in RADAFII nanofibers, the steric hindrance effect weakened so that the guest lipophilicity dominated release behaviors. PR, having highest lipophilicity, could more stably locate in hydrophobic area of the peptide nanofiber in the RADAFII hydrogel network. The probability that it was detached from the network was therefore much lower than other two molecules.

On the basis of the striking different releases of these two peptide scaffolds, we suggested that guest size and lipophilicity influenced the release competitively. The release of RADAFl system was dominated by guest size, and the guest lipophilicity controlled the release behavior in RADAFII system (Fig. 8).

As seen, the release curves in Fig. 7 revealed an initial burst release during the early stage, which could be explained by the molecules that located in the interspaces of network but not bound to the peptide nanofibers. Guest entrapped as a free molecule in the scaffold (guests with arrows in Fig. 8) was quickly diffused into the release media, and consequently, the initial burst release was observed. To understand the dynamics of drug release from the hydrogels, the first half of release ratios was plotted against the square root of releasing time (Fig. 9). A good linear relationship was found, indicating that the mechanism of the release of the guest molecule should be Fickian diffusion control [6,11,21,28].

Diffusion coefficients were calculated from the slope of this straight line for each of the substances within each of the hydrogels (Table 1). Here, the diffusion coefficients of various guests were evidently different from each other. For RADAFl hydrogels, it was observed that diffusion

Fig. 5. Storage modulus (G' , black) and loss modulus (G'' , gray) as time sweeps for various peptide RADAFl and RADAFII scaffolds: (a) RADAFl scaffold, (b) RADAFl scaffold loading Phe, (c) RADAFl scaffold loading Trp, (d) RADAFl scaffold loading PR, (e) RADAFII scaffold, (f) RADAFII scaffold loading Phe, (g) RADAFII scaffold loading Trp, and (h) RADAFl scaffold loading PR. The concentrations of peptide and guest were 0.5 (w/v)% and 1 mM, respectively.

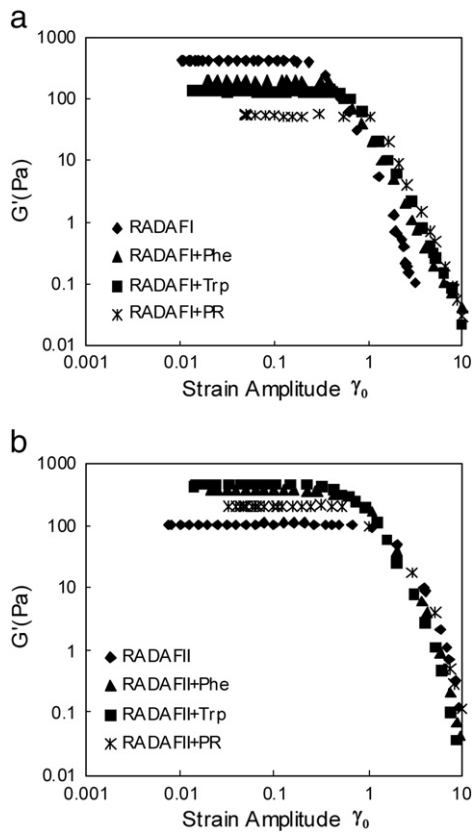


Fig. 6. Storage modulus (G') as strain sweeps for various (a) RADAFI and (b) RADAFII scaffolds. The concentrations of peptide and guest were 0.5 (w/v)% and 1 mM, respectively.

coefficients enhanced with increasing the guest size. However, for RADAFII systems, decreasing guest size facilitated its detachment and diffusion. These results were similar to those observed elsewhere for other gel-based delivery systems, where selective permeability and release had been reported [6]. These peptides could be expected to self-assemble into nanofiber scaffolds with π - π stacking [20], which influenced diffusion of the guest molecules purely on the basis of its

Table 1
Summary of some parameters of various peptide scaffolds.

Code	Peptide	Guest	Strain recovery ^a (after 3 min)	Equilibrium release ratio	Diffusion coefficient ^b , [21] ($\times 10^{-10}$, $m^2 s^{-1}$)
RADAFI	RADAFI	–	95%	–	–
RADAFI + Phe	RADAFI	Phenylalanine	92%	0.22	0.159
RADAFI + Trp	RADAFI	Tryptophan	94%	0.34	0.385
RADAFI + PR	RADAFI	Phenol red	92%	0.48	0.672
RADAFII	RADAFII	–	83%	–	–
RADAFII + Phe	RADAFII	Phenylalanine	83%	0.17	0.110
RADAFII + Trp	RADAFII	Tryptophan	85%	0.12	0.031
RADAFII + PR	RADAFII	Phenol red	82%	0.07	0.008

^a A ratio of G' after strain amplitude sweep test and then 3 min to G' before strain test.

^b Diffusion coefficients were calculated from the linear slope of the plots of release ratio versus $t^{1/2}$ in Fig. 9.

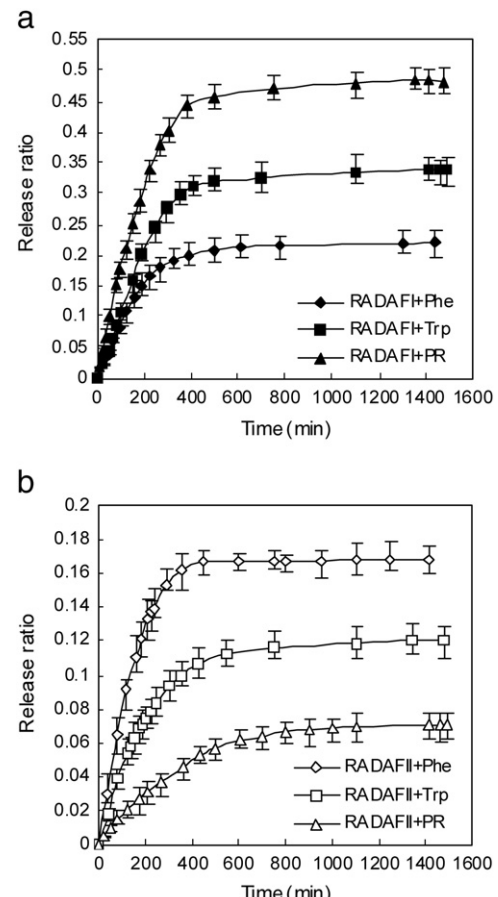


Fig. 7. Time courses of guest release from hydrogel systems of peptide (a) RADAFI and (b) RADAFII. The data represents an average of five repeats. The concentrations of peptide and guest were 0.5 (w/v)% and 1 mM, respectively.

size. This resulted in the observations that the guests with different dimensions had quite different diffusion coefficients, which could contribute to new delivery systems.

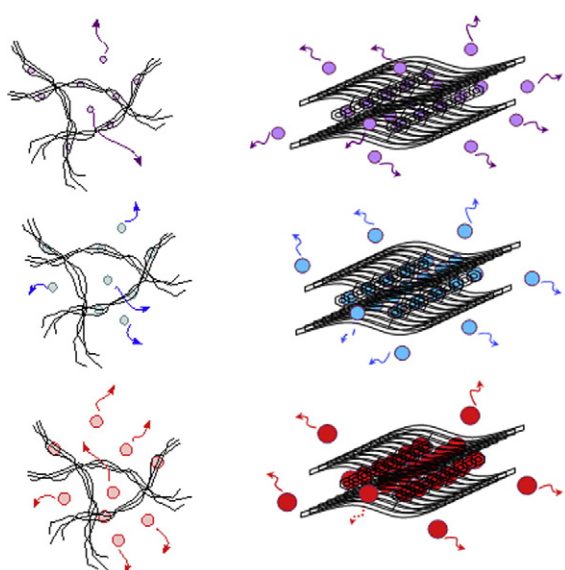


Fig. 8. Schematic view of the guest locations in peptides (left) RADAFI and (right) RADAFII hydrogels: (top) Phe, (middle) Trp, and (bottom) PR. Arrows showed guests located in the interspaces of network as free molecules, which could be quickly released.

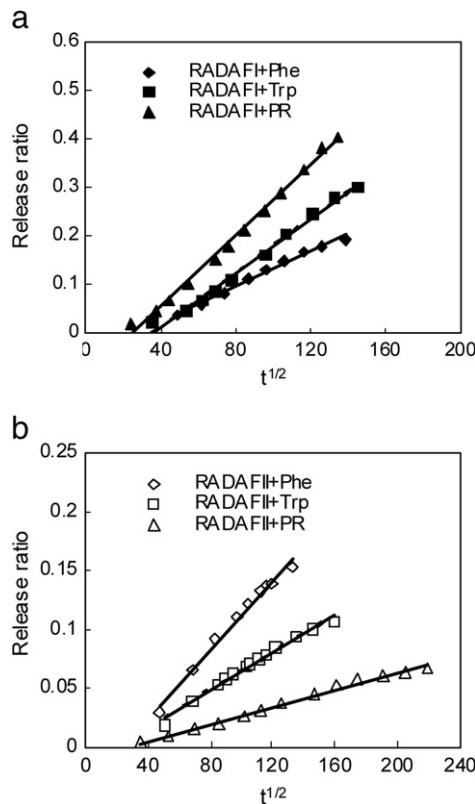


Fig. 9. Plots of release ratio as a function of $t^{1/2}$ for the guests released from the (a) RADAFl and (b) RADAFII hydrogels.

4. Conclusions

In summary, an attempt was made to rationally control release via the selection of appropriate building blocks and guests. Hydrogels could be prepared from peptide RADAFl and RADAFII, containing the same amino acid compositions but different positions of one phenylalanine residue, by self-association of peptide nanofibers to controllably alter the physical properties of the hydrogel materials. CD experiments favored a β -sheet structure of these gelators in their respective hydrogel state. Self-assembly of the peptides into nanofibers with distinct nanoarchitectures and physical morphology of the interconnected nanofibrillar network structures were observed by AFM images. Moreover, the hydrogels could hold and release model guests selectively, which might be beneficial for using these peptide supramolecular hydrogels as a drug delivery vehicle. Release kinetics emphasized that the systems were under Fickian diffusion control. Furthermore, the obtained release function would be modulated by both rational design of the peptides used for hydrogel formation and choice of the entrapped molecules. Altogether, we testified the suitability of these two peptide hydrogels for encapsulation and release of some guests with various sizes to confirm that the scaffolds developed within this work displayed potential as *in situ* soft materials for tissue engineering and drug delivery applications.

Acknowledgements

The authors acknowledge the International Graduate Program 2007 in Nagoya Institute of Technology funded by Japanese Government. We thank Prof. Shuguang Zhang (Massachusetts Institute of Technology) and Dr. Hidenori Yokoi (Menicon Co., Ltd.) for helpful discussion. We also thank Dr. Sohei Abiko and Ass. Prof. Kenji Nagata for experimentation support, and finally, members of the Kinoshita Laboratory for help.

Appendix A. Supplementary data

Supplementary data to this article can be found online at doi:10.1016/j.conrel.2010.08.002.

References

- [1] A.O. Boztas, A. Guiseppe-Elie, Immobilization and release of the redox mediator ferrocene monocarboxylic acid from within cross-linked p(HEMA-co-PEGMA-co-HMMA) hydrogels, *Biomacromolecules* 10 (2009) 2135–2143.
- [2] K.A. George, E. Wentrup-Byrne, D.J.T. Hill, A.K. Whittaker, Investigation into the diffusion of water into HEMA-co-MOEP hydrogels, *Biomacromolecules* 5 (2004) 1194–1199.
- [3] T. Vermonden, S.S. Jena, D. Barriet, R. Censi, J. van der Gucht, W.E. Hennink, et al., Macromolecular diffusion in self-assembling biodegradable thermosensitive hydrogels, *Macromolecules* 43 (2010) 782–789.
- [4] W.E. Hennink, C.F. van Nostrum, Novel crosslinking methods to design hydrogels, *Adv. Drug Deliv. Rev.* 54 (2002) 13–36.
- [5] M. Teodorescu, A. Lungu, P.O. Stanescu, C. Neamtu, Preparation and properties of novel slow-release NPK agrochemical formulations based on poly(acrylic acid) hydrogels and liquid fertilizers, *Ind. Eng. Chem. Res.* 48 (2009) 6527–6534.
- [6] S. Sutton, N.L. Campbell, A.I. Cooper, M. Kirkland, W.J. Frith, D.J. Adams, Controlled release from modified amino acid hydrogels governed by molecular size or network dynamics, *Langmuir* 25 (2009) 10285–10291.
- [7] M. de Loos, B.L. Feringa, J.H. van Esch, Design and application of self-assembled low molecular weight hydrogels, *Eur. J. Org. Chem.* 2005 (2005) 3615–3631.
- [8] L.A. Estroff, A.D. Hamilton, Water gelation by small organic molecules, *Chem. Rev.* 104 (2004) 1201–1218.
- [9] P. Dastidar, Supramolecular gelling agents: can they be designed? *Chem. Soc. Rev.* 37 (2008) 2699–2715.
- [10] J. Naskar, G. Palui, A. Banerjee, Tetrapeptide-based hydrogels: for encapsulation and slow release of an anticancer drug at physiological pH, *J. Phys. Chem. B* 113 (2009) 11787–11792.
- [11] L. Chen, J. Wu, L. Yuwen, T. Shu, M. Xu, M. Zhang, et al., Inclusion of tetracycline hydrochloride within supramolecular gels and its controlled release to bovine serum albumin, *Langmuir* 25 (2009) 8434–8438.
- [12] H. Tai, D. Howard, S. Takae, W. Wang, T. Vermonden, W.E. Hennink, et al., Photo-cross-linked hydrogels from thermoresponsive PEGMEMA-PPGMA-EGDMA copolymers containing multiple methacrylate groups: mechanical property, swelling, protein release, and cytotoxicity, *Biomacromolecules* 10 (2009) 2895–2903.
- [13] A. Khademhosseini, R. Langer, Microengineered hydrogels for tissue engineering, *Biomaterials* 28 (2007) 5087–5092.
- [14] N.A. Peppas, J.Z. Hilt, A. Khademhosseini, R. Langer, Hydrogels in biology and medicine: from molecular principles to bionanotechnology, *Adv. Mater.* 18 (2006) 1345–1360.
- [15] H. Byssell, A. Schmidtchen, M. Malmsten, Binding and release of consensus peptides by poly(acrylic acid) microgels, *Biomacromolecules* 10 (2009) 2162–2168.
- [16] A. Besheer, K.M. Wood, N.A. Peppas, K. Mäder, Loading and mobility of spin-labeled insulin in physiologically responsive complexation hydrogels intended for oral administration, *J. Control. Release* 111 (2006) 73–80.
- [17] Y. Li, R. de Vries, T. Slaghek, J. Timmermans, M.A. Cohen Stuart, W. Norde, Preparation and characterization of oxidized starch polymer microgels for encapsulation and controlled release of functional ingredients, *Biomacromolecules* 10 (2009) 1931–1938.
- [18] M.C. Branco, D.J. Pochan, N.J. Wagner, J.P. Schneider, Macromolecular diffusion and release from self-assembled β -hairpin peptide hydrogels, *Biomaterials* 30 (2009) 1339–1347.
- [19] H. Komatsu, S. Matsumoto, S. Tamaru, K. Kaneko, M. Ikeda, I. Hamachi, Supramolecular hydrogel exhibiting four basic logic gate functions to fine-tune substance release, *J. Am. Chem. Soc.* 131 (2009) 5580–5585.
- [20] Y. Zhao, M. Tanaka, T. Kinoshita, M. Higuchi, T. Tan, Nanofibrous scaffold from self-assembly of β -sheet peptides containing phenylalanine for controlled release, *J. Control. Release* 142 (2010) 354–360.
- [21] Y. Zhao, M. Tanaka, T. Kinoshita, M. Higuchi, T. Tan, Controlled release and entrapment of enantiomers in self-assembling scaffolds composed of β -sheet peptides, *Biomacromolecules* 10 (2009) 3266–3272.
- [22] Y. Zhao, H. Yokoi, M. Tanaka, T. Kinoshita, T. Tan, Self-assembled pH-responsive hydrogels composed of the RATEA16 peptide, *Biomacromolecules* 9 (2008) 1511–1518.
- [23] Y. Zhao, T. Tan, H. Yokoi, M. Tanaka, T. Kinoshita, Controlled release and interaction of protein using self-assembling peptide RATEA16 nanofiber hydrogels, *J. Polym. Sci. Pol. Chem.* 46 (2008) 4927–4933.
- [24] Y. Wang, D. Xin, K. Liu, M. Zhu, J. Xiang, Heparin-paclitaxel conjugates as drug delivery system: synthesis, self-assembly property, drug release, and antitumor activity, *Bioconjug. Chem.* 20 (2009) 2214–2221.
- [25] K.Y. Win, S.S. Feng, In vitro and in vivo studies on vitamin E TPGS-emulsified poly (D, L-lactic-co-glycolic acid) nanoparticles for paclitaxel formulation, *Biomaterials* 27 (2006) 2285–2291.
- [26] R.A. Hule, R.P. Nagarkar, B. Hammouda, J.P. Schneider, D.J. Pochan, Dependence of self-assembled peptide hydrogel network structure on local fibril nanostructure, *Macromolecules* 42 (2009) 7137–7145.
- [27] J.N. Sheria, X.S. Sun, Effect of peptide sequence on surface properties and self-assembly of an amphiphilic pH-responsive peptide, *Biomacromolecules* 10 (2009) 2446–2450.

- [28] Y. Nagai, L.D. Unsworth, S. Koutsopoulos, S. Zhang, Slow release of molecules in self-assembling peptide nanofiber scaffold, *J. Control. Release* 115 (2006) 18–25.
- [29] L. Hsu, G.L. Cvetanovich, S.I. Stupp, Peptide amphiphile nanofibers with conjugated polydiacetylene backbones in their core, *J. Am. Chem. Soc.* 130 (2008) 3892–3899.
- [30] H. Shao, J.W. Lockman, J.R. Parquette, Coupled conformational equilibria in β -sheet peptide-dendron conjugates, *J. Am. Chem. Soc.* 129 (2007) 1884–1885.
- [31] R. Orbach, L. Adler-Abramovich, S. Zigeron, I. Mironi-Harpaz, D. Seliktar, E. Gazit, Self-assembling Fmoc-peptides as a platform for the formation of nanostructures and hydrogels, *Biomacromolecules* 10 (2009) 2646–2651.
- [32] J.M. Anderson, A. Andukuri, D.J. Lim, H.W. Jun, Modulating the gelation properties of self-assembling peptide amphiphiles, *ACS Nano* 3 (2009) 3447–3454.
- [33] J.K. Kim, J. Anderson, H.W. Jun, M.A. Repka, S. Jo, Self-assembling peptide amphiphile-based nanofiber gel for bioresponsive cisplatin delivery, *Mol. Pharm.* 6 (2009) 978–985.
- [34] C.J. Bowerman, D.M. Ryan, D.A. Nissan, B.L. Nilsson, The effect of increasing hydrophobicity on the self-assembly of amphipathic β -sheet peptides, *Mol. Biosyst.* 5 (2009) 1058–1069.
- [35] L. Aulisa, H. Dong, J.D. Hartgerink, Self-assembly of multidomain peptides: sequence variation allows control over cross-linking and viscoelasticity, *Biomacromolecules* 10 (2009) 2694–2698.
- [36] A. Aggelis, M. Bell, L.M. Carrick, C.W.G. Fishwick, R. Harding, P.J. Mawer, et al., pH as a trigger of peptide β -sheet self-assembly and reversible switching between nematic and isotropic phases, *J. Am. Chem. Soc.* 125 (2003) 9619–9628.
- [37] E. Beniash, J.D. Hartgerink, H. Storrie, J.C. Stendahl, S.I. Stupp, Self-assembling peptide amphiphile nanofiber matrices for cell entrapment, *Acta Biomater.* 1 (2005) 387–397.
- [38] R.V. Rughani, D.A. Salick, M.S. Lamm, T. Yucel, D.J. Pochan, J.P. Schneider, Folding, self-assembly, and bulk material properties of a de novo designed three-stranded β -sheet hydrogel, *Biomacromolecules* 10 (2009) 1295–1304.
- [39] L. Haines-Butterick, K. Rajagopal, M. Branco, D. Salick, R. Rughani, M. Pilarz, et al., Controlling hydrogelation kinetics by peptide design for three-dimensional encapsulation and injectable delivery of cells, *Proc. Natl. Acad. Sci. U.S.A.* 104 (2007) 7791–7796.
- [40] J. Wang, S. Han, G. Meng, H. Xu, D. Xia, X. Zhao, et al., Dynamic self-assembly of surfactant-like peptides A_6K and A_9K , *Soft Matter* 5 (2009) 3870–3878.
- [41] G. Palui, A. Garai, J. Nanda, A.K. Nandi, A. Banerjee, Organogels from different self-assembling new dendritic peptides: morphology, rheology, and structural investigations, *J. Phys. Chem. B* 114 (2010) 1249–1256.